NUMERICAL STUDY OF HEAT TRANSFER IN TURBULENT FLOWS, WITH APPLICATION

Laura Alina STIKA *, **Valeriu Alexandru VILAG ***, **Mircea BOSCOIANU ****, **Gheorghe MEGHERELU ***

*Romanian Research and Development Institute for Gas Turbines COMOTI,
**"Henry Coandă" Air Force Academy, Brasov, Romania

Abstract: This paper describes a numerical method for analyzing the heat transfer, in a hot section of a turbo shaft. The high temperatures of the struts behind a free turbine are transferred, through conduction, to the casing of the free turbine's shaft. In this way, there is a risk of overheating the oil inside this casing. To reduce this risk, on the casing can be added a part, crossed by a mass flow of cool air. The application focuses on the performance of this cooling part. In order to study the heat transfer from the strut to the oil housing, several computations were performed, using the CFD software Ansys CFX. Several cases were analyzed, by slightly modifying the geometry, as well as the air mass flow passing through the analyzed part. The different results were compared, the best configuration in terms of cooling efficiency being the one predicted by the theory.
Keywords: heat transfer; CFD; cooling.

1. INTRODUCTION

In gas turbines, lubrication systems usually have two functions [1]: to oil and to cool the regions between rotating and stationary bearing surfaces.

In order to function properly, the oil must be kept under a maximum admissible temperature; therefore the majority of the gas turbine's lubrication systems include oil coolers [1].

Although the oil coolers are efficient, they are only required to remove the heat from the oil before it is re-introduced into the gas turbine.

In other words, they aren't designed to protect the lubricant along its route inside the gas turbine, thus there is a possibility for the oil to encounter hot surfaces that could increase its temperature to more than the admissible one.

In this case, additional cooling solutions must be applied.

This paper focuses on one of these solutions, which consists in adding a component on the casing of a power turbine's shaft, highlighted in Fig. 1.
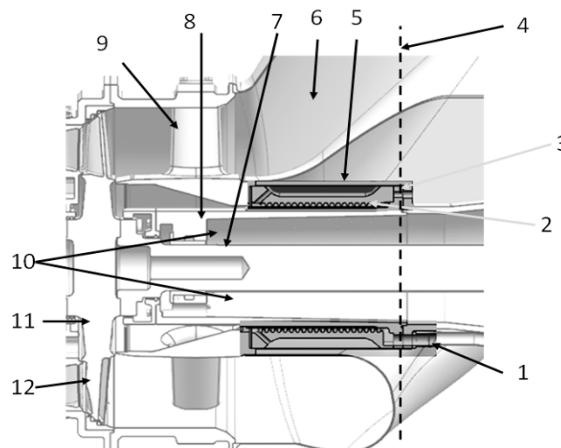

Fig. 1- Schematics of the cooling part and its position. 1-Air inlet; 2- The helically coiled passage; 3- Contact surface between the cooling part and the shaft's casing (the "measure wall"); 4-"Measure wall's" position; 5- Position of the air outlet; 6- Exhaust system of the turboshaft; 7- The power turbine's shaft; 8- The shaft's casing; 9- Strut; 10- Region with oil, surrounding the shaft; 11- Power turbine's disk; 12- Power turbine's blade.

This element prevents the transfer of high temperatures form the struts to the oil.

Concerning its geometry, the part is a hollow cylinder crossed by a mass flow of cool air, which follows a helically coiled path, with a trapezoidal cross-section. The coiled form was chosen based on its good results in terms of heat transfer of the coiled tubes [2], hence their wide variety of applications like chemical process reactors and industrial marine boilers [2].

2. DATA BASE AND METHOD

2.1 Method. The numerical simulations provided the temperature transferred to the shaft's casing, the temperature distribution on the domain walls and also information about the flow inside the part. The maximum temperature and its distribution on the "measure wall" - presented in Fig. 1 - were analyzed for each case. This parameter was considered to best describe the performance of the cooling part.

Table 1. Configuration and boundary conditions for the numerical simulations.

C	Geom type	Inlet		Outlet	Solid
		p* [bara]	T* [°C]	p [bara]	Mat
1	1 coil	1.5	30	1.1	STL
2	1 coil	2	30	1.1	STL
3	3 coils	1.5	30	1.1	STL
4	3 coils	2	30	1.1	STL
5	3 coils	2.3	30	1.1	STL
6	3 coils	2	30	1.1	S/S

Where C- Case number, Geom- geometry, p*- total pressure, T*- total temperature, p- static pressure, mat- material, STL- steel, S/S - stainless steel.

Regarding the geometry, the part analyzed has a hollow cylindrical form, with a length of 193 mm, an exterior radius of 113 mm, for geometry type with 1 coil and an exterior radius of 115 mm for the geometry type with 3 coils and an interior radius of 81.5 mm.

For the geometry type with 3 coils, the exterior radius was enlarged by 2 mm, due to mesh issues.

This change was made only on the solid domain; the fluid domain in that specific region is the same for the two types of geometries. It is assumed that this change doesn't influence the configuration in an optimistic manner, in other words, adding some more material in that specific area, it will make the exterior solid wall thicker, thus harder to cool.

The path of the airflow can be observed in Fig. 2 and in Fig. 3. The only differences between the two types of geometries are the number of coils and the enlarged radius earlier presented.
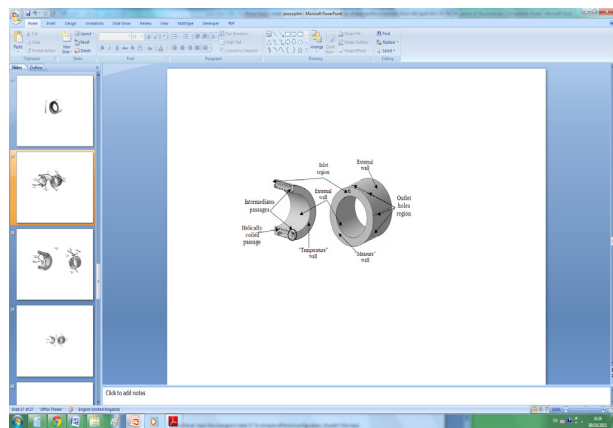

Fig. 2- Solid block domain used for the simulations (left: view of half of the domain; right- isometric view)

The fluid enters the domain through the circular inlet surface of radius 7 mm; crosses the trapezoidal cross-section of 36 mm2 area coil or coils; passes through the 6 intermediates 3 mm radius cylindrical holes and then exits through the outlet which consists in 8 cylindrical, 5 mm radius holes.
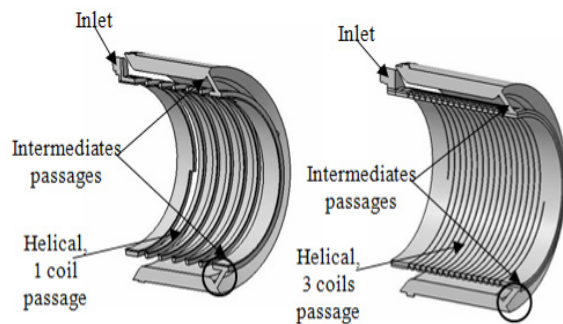

Fig. 3- Half of the fluid block domain, for the two types of geometry (left: one coil geometry; right- 3 coils geometry)

The numerical simulations have been carried out in the Reynolds Averaged Navier Stokes (RANS) formulation, using the Ansys CFX commercial software. For each type of geometry a computational domain containing two blocks (a solid one and a fluid one) -presented in Fig. 2 and Fig. 3- was defined. These domains were meshed by means of an unstructured grid into 1706426 tetrahedral computational cells, resulting in 414074 nodes for the one coil geometry and 2186629 tetrahedral computational cells, resulting in 498733 nodes for the three coils geometry.

The following boundary conditions were applied on the surfaces indicated in Fig. 2 and Fig. 3, for each of the 6 numerical simulations.

Inlet: Subsonic inlet boundary conditions with the total pressures in Table 1 and a temperature of 30 °C.

Outlet: Subsonic outlet boundary condition with the static pressure in Table 1.

"Temperature" wall: Wall with fixed temperature of 600 °C.

"Measure" wall: Solid, no-slip, adiabatic wall.

External wall: Solid, no-slip adiabatic wall.

The walls surrounding the fluid were set as interfaces between the fluid and the solid blocks, except for the inlet and outlet surfaces.

The fluid for all the numerical simulation computations was set to Air Ideal Gas, with a reference pressure of 1 atm.

For the solid domain, steel was used for the first five numerical simulations and stainless steel for the last one. The properties of these materials are presented in Table 2.

Table 2. Proprieties of the materials used in the numerical simulations.

Proprieties	Steel	Stainless steel
Molar mass [kg/mol]	55.85	55.91
Density [kg/ m³]	7854	7900
Specific heat capacity [J/ (kg*K)]	434	500
Thermal conductivity [W/(m*K)]	60.5	15 [3]

In the first attempt to carry out the simulations with the inlet and outlet boundary conditions presented above, because of the solver numerical characteristics [4], as the solution progressed, reversed flow occurred at the outlet and at the inlet boundary. To work around this, the CFX-solver tried enforcing the flow by creating artificial walls at the entry and the exit of the domain [4], which caused a solver failure. To solve this, the numerical simulations were initialized by another set of numerical simulations, where all the inlet and outlet boundaries were set as openings. Once the solutions of the initialization numerical simulations (with the inlet and outlet boundary conditions set as openings) converged, the solver was restarted and the original, inflow and outflow, boundary conditions were restored. As it is stated in [4], if the problem doesn't persists after changing the boundary conditions from "opening" type to "inlet/outlet", the error isn't in the case definition. Basically, the first simulations were only used to calculate initial conditions for the computations presented in this paper. After the boundary conditions have been restored, the solver no longer had an abnormal behavior, which indicates that the location of the inlet and outlet was set properly, meaning that they are not located in a recirculation zone.

The simulations were carried out until convergence of the results was reached. The convergence criterion was a Normalized Residual level of the order 10-5 [4].

2.2 Results. In order to analyze the performance of the configurations presented, a target was set. The function of the cooling part is to prevent high temperatures from the struts to reach the oil inside the shaft's casing and therefore the obvious target was chosen based on the operating oil temperature. In high temperature applications, synthetic lubricants are used at temperatures up to 175 °C [1], therefore the studied element should transfer to the shaft's casing a temperature lower than this value. This means that if in the studied application the averaged temperature on the "measure" wall defined earlier, is lower than 175 °C, the cooling part fulfills its purpose.

The results are presented, for all 6 cases, in Table 3.

Table 3. Averaged numerical simulation results.

C	"M" Wall T [°C]	Outlet T* [°C]	Outlet v [m/s]	Inlet v [m/s]	Fluid domain $\dot{M}$ [kg/s]
1	505.4	585.4	6.4	5.6	0.001349
2	355.1	534.4	12.5	9.8	0.003454
3	485.4	590.7	22.3	17.9	0.004751
4	237.4	504.3	40.8	30.9	0.01089
5	184.8	421.6	47.5	34.9	0.014126
6	156.4	380.0	39.0	35.0	0.012553

The first analyzed case was the reference, Case 1, configuration. First, the velocity vectors were checked to ensure that the phenomenon of inflow at the outlet boundary and outflow at the inlet boundary hadn't occurred. As it can be seen in Fig. 4, the velocity vector is towards inside the domain at the inlet and towards the exit at the outlet.

The second check was to verify the temperature after the intermediate circular passage. Although this temperature was higher than at the outlet, the difference was small, of about 17°C, so the geometry surrounding the fluid, after the intermediate passage, was kept the same for all 6 cases. This phenomenon of cooling the air after the intermediate passage no longer occurs in the three coils configurations where the mass flow is increased.

The total temperature of the outlet surface is only with 15 °C lower than the one imposed on the "temperature" wall, which illustrates the fact that this configuration is working, though, as seen in the Table 3, it gave poor results compared with the imposed target. The difference between the so called "temperature" wall and "measure" wall was of only 100 °C which means that to increase the element's performance it is required to enhance the heat transfer.

In general, there are two types of techniques to enhance the heat transfer, in this configuration: active and passive techniques [5]. The active techniques require external forces, while the passive techniques require geometry or material changes [5]. Both techniques were used in this study.
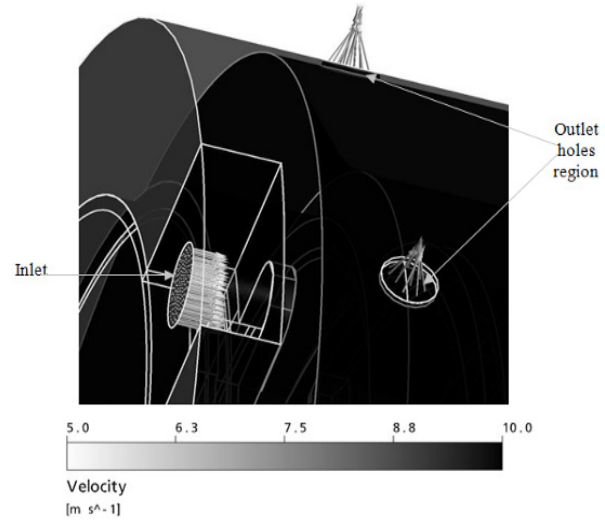

Fig. 4- Velocity vector at: inlet and on two surfaces of the outlet, for the Case 1.

In numerical simulations, the easiest and fastest way to get results is using the active techniques, namely increasing the total pressure at inlet boundary and thus the cool air mass flow.

For the Case 2, the total absolute pressure at the inlet boundary was increased at 2 bara, as seen in Table 1, but it still wasn't enough to reach the desired temperature on the "measure" wall.

The same phenomenon occurred as in the first case, namely the averaged total temperature of the fluid after the intermediate passages was a little higher than the averaged total temperature at the outlet. As seen in Fig. 5, this cooling of the air doesn't have a considerable consequence on the averaged temperature of the "measure" wall.

The contact surface between fluid and solid domain is proportional with the heat transfer [2]. Hence, to further improve the performance of the cooling part, this surface was increased. In this way, the 3 coils geometry resulted, as presented in Fig. 3 and used in the Cases 3, 4, 5 and 6.

As in the configurations with one coil, the total pressure on the inlet boundary was increased from 1.5 bara, this time up to the value of 2.3 bara.
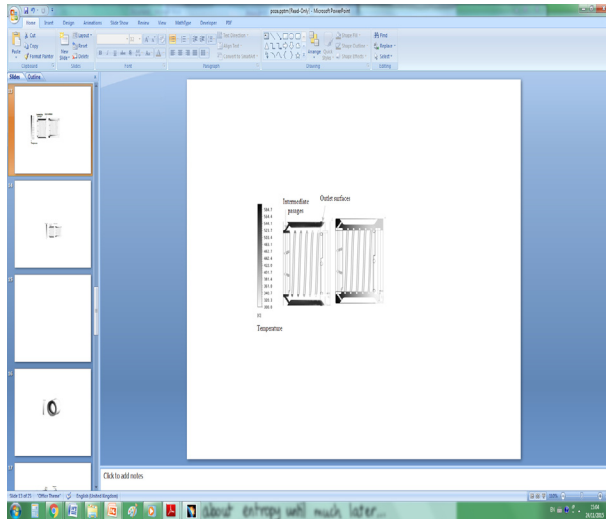

Fig. 5- Temperature distribution on the mid-section plane, for Case 2 (on the left: fluid domain; on the right solid domain)

The best result, using steel as material for the solid domain, is obviously the Case 5, with the total pressure boundary condition of 2.3 bara, resulting in the greatest air mass flow of all 6 cases. Still, the recorded temperature was 10 °C above the target.

As in the configurations with one coil, the total pressure on the inlet boundary was increased from 1.5 bara, this time up to the value of 2.3 bara. The best result, using steel as material for the solid domain, is obviously the Case 5, with the total pressure boundary condition of 2.3 bara, resulting in the greatest air mass flow of all 6 cases. Still, the recorded temperature was 10 °C above the target.

Also it can be noticed that, for the Case 3 the air mass flow is little higher than the one from Case 2, even though Case 2 has a higher inlet pressure, and both cases have the same inlet area (as it is known, a mass flow is related to the density, velocity of the fluid and area through which the fluid passes [6]). This can be explained by the fact that the air mass flow is proportional to the narrowest area of the air path [6], that being, in this case, the entrance in the helically coiled passage.

For Case 3 (geometry with 3 coils) the narrowest area is three times bigger than for Case 1 (geometry with 1 coil).

Hence, increasing this area had more effect in terms of air mass flow than changing the inlet total pressure.

The solution used in Case 6 was changing the material. In the numerical case, the properties of the solid domain were changed according to those showed in Table 2, for stainless steel. It is worth noting that there are big differences between the thermal conductivity coefficients of steel, of 60 W/(m*K), and of stainless steel, of 15 W/(m*K) [3]. This distinction between the proprieties of the two materials led to a global difference of 81 °C, in terms of averaged temperature. The plotted temperature on the solid domain used in Case 6 is presented in Fig. 6. It can be noticed that, on the region of interest, respectively the "measure" wall, the temperature is smaller near the inlet area and increases until the maximum value obtained in the diametrically opposed point. To obtain an uniform distribution, another inlet placed in the hottest region of the "measure" wall is required.
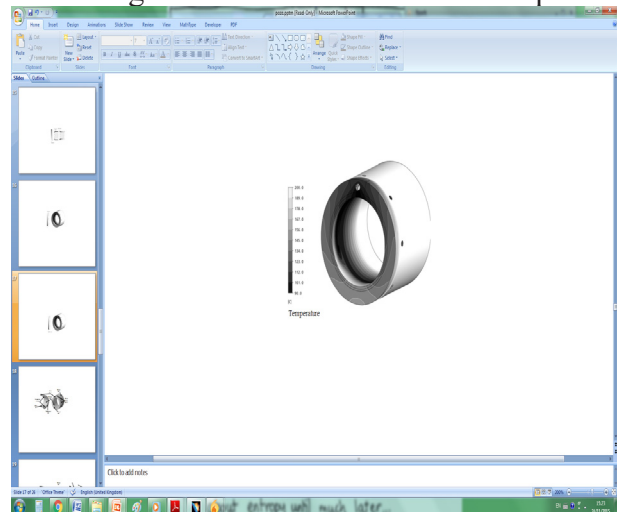

Fig. 6- Temperature distribution on the solid domain for Case 6

CONCLUSIONS

Several geometrical configurations, materials and inlet pressures were analyzed in order to select the best configuration for the cooling part used that prevents the transfer of high temperatures form the struts to the oil in a turboshaft.

Compared to the reference configuration (Case 1), it was found that only increasing the inlet pressure from 1.5 to 2 bara was not enough to reach the desired temperature on the "measure" temperature wall, even though an improvement was achieved.

Next, the geometrical configuration of the cooling part was modified, by raising the number of coils from 1 to 3, and raising the inlet pressure from 1.5 to 2 and finally to 2.3 bara. It was found that the 2.3 bara Case 5 provides the highest cooling mass flow, but still failing to meet the temperature requirements.

Finally, the cooling part material was changed from steel to stainless steel. It was found that for the three coils geometry, even the cooling flow provided by a 2 bara inlet pressure is sufficient to meet the temperature requirements.

BIBLIOGRAPHY

[1] Tony Giampaolo *Gas Turbine Handbook - Principles and Practices* 3rd Edition, MSME, PE, (2006),

[2] Adrian Bejan, Allan D. Kraus - *Heat transfer handbook*,chapter 14 *Heat transfer enhancement*, John Wiley & Sons (2003),

[3] Standard : EN 10088-1:2005 *Stainless steels- list of stainless steels* (2005),

[4] ANSYS, Inc Southpointe *CFX Solver modeling-User guide*, (2013),

[5] Paisarn Naphon, Somchai Wongwises *A review of flow and heat transfer characteristics in curved tubes*, (2004)

[6] E. Carafoli, V.N. Constantinescu: *Dinamica fluidelor incompresibile (I)* Editura Academiei, Bucuresti, 1981.

[7] ANSYS, Inc Southpointe *CFX Solver modeling-User guide*, (2013),

[8] Adrian Bejan, Allan D. Kraus - *Heat transfer handbook*,chapter 14 *Heat transfer enhancement*, John Wiley & Sons (2003),

[9] E. Carafoli, V.N. Constantinescu: *Dinamica fluidelor incompresibile (I)* Editura Academiei, Bucuresti, 1981,

[10] Tony Giampaolo *Gas Turbine Handbook - Principles and Practices* 3rd Edition, MSME, PE, (2006),

[11] Paisarn Naphon, Somchai Wongwises *A review of flow and heat transfer*

[12] Standard: EN 10088-1:2005 *Stainless steels- list of stainless steels* (2005).